Chem. Mater. **2008,** *20,* 2081–2085

Articles

A Library of Single-Crystal Metal−Tin Nanorods: Using Diffusion as a Tool for Controlling the Morphology of Intermetallic Nanocrystals

Nam Hawn Chou and Raymond E. Schaak*

Department of Chemistry, The Pennsylvania State University, 104 Chemistry Building, University Park, Pennsylvania 16802

Received December 20, 2007. Revised Manuscript Received January 18, 2008

We describe a unified and general template-based strategy for synthesizing a library of morphology-controllable *M*−Sn (*M* = Co, Ni, Cu, Ag, Au, Pt, Ru) intermetallic nanorods. The reaction of β-Sn nanorod templates with appropriate metal salt solutions under reducing conditions yields single-crystal intermetallic nanorods of $CoSn_3$, Ni_3Sn_4, Cu_6Sn_5, Ag_4Sn, AuSn, PtSn, and $RuSn_2$. Temperature plays a key role in maintaining the morphology of the β-Sn nanorod templates in the final *M*−Sn products and also selectively generating spherical nanocrystals vs dense nanorods vs hollow nanorods, in some cases (e.g., $CoSn_3$) within the same system. These observations are linked to the diffusion process, and accordingly, the melting points of the transition elements used in this study can help us understand and predict the morphologies that can be formed, as well as the lowest temperature at which a particular intermetallic compound can form using low-temperature solution routes.

Introduction

Intermetallic compounds of the late transition metals form over a range of compositions and adopt many different crystal structures. This compositional and structural diversity makes intermetallics important and versatile materials for a variety of applications, including superconductors,[1] magnets,[2] shape memory alloys,[3] hydrogen storage materials,[4] catalysts,[5] and electrodes.[6] However, because of this chemical diversity, synthesizing nanocrystalline intermetallic compounds with controlled shapes and sizes can be difficult. The methods typically used to rigorously control nanocrystal morphology use ligands, surfactants, or polymers that tend to bind preferentially to one or more surfaces, thereby limiting growth in certain directions and leading to nanocrystals with well-defined shapes.[7] Finding the appropriate combination of surfactants to facilitate shape-controlled growth in nanocrystalline intermetallic systems is not impossible,[8] but remains rare and can be difficult to generalize to other systems.

Here, we describe a general template-based strategy for synthesizing a library of morphology-controlled *M*−Sn (*M* = Co, Ni, Cu, Ag, Au, Pt, Ru) intermetallic nanorods. This work builds significantly on results reported by several groups in the past few years involving the use of nanocrystal templates to generate derivative nanocrystals via a diffusion mechanism. For example, researchers have been able to synthesize Ag_2Se nanowires by reacting Se nanowires with a solution of $AgNO_3$,[9] as well as a variety of hollow metal sulfides,[10] phosphides,[11] and oxides[12] using reactions that employ a nanoscale Kirkendall effect. Some intermetallic

---

* Corresponding author. E-mail: schaak@chem.psu.edu.

(1) (a) Cava, R. J.; Zandbergen, H. W.; Krajewski, J. J.; Peck, W. F.; Siegriest, T.; Batlogg, B.; Vandover, R. B.; Felder, R. J.; Mizuhashi, K.; Lee, J. O.; Eisaki, H.; Uchida, S. *Nature* **1994**, *367*, 252. (b) Buzea, C.; Yamashita, T. *Supercond. Sci. Technol.* **2001**, *14*, R115. (c) Godeke, A. *Supercond. Sci. Technol.* **2006**, *19*, R68. (d) He, T.; Huang, Q.; Ramirez, A. P.; Wang, Y.; Regan, K. A.; Rogado, N.; Hayward, M. A.; Haas, M. K.; Slusky, J. S.; Inumara, K.; Zandbergen, H. W.; Ong, N. P.; Cava, R. J. *Nature* **2001**, *411*, 54.

(2) (a) Sun, S.; Murray, C. B.; Weller, D.; Folks, L.; Moser, A. *Science* **2000**, *287*, 1989. (b) Sun, S. *Adv. Mater.* **2006**, *18*, 393. (c) Burzo, E. *Rep. Prog. Phys.* **1998**, *61*, 1099. (d) Hadjipanayis, G. C. *J. Magn. Magn. Mater.* **1999**, *200*, 373.

(3) (a) Wuttig, M.; Liu, L.; Tsuchiya, K.; James, R. D. *J. Appl. Phys.* **2000**, *87*, 4707. (b) Otsuka, K.; Ren, X. B. *Intermetallics* **1999**, *7*, 511.

(4) (a) Kirchheim, R.; Mutschele, T.; Keininger, W.; Gleiter, H.; Birringer, R.; Koble, T. D. *Mater. Sci. Eng.* **1998**, *99*, 457. (b) Bououdina, M.; Grant, D.; Walker, G. *Int. J. Hydrogen Energy* **2006**, *31*, 177. (c) Cohen, R. L.; Wernick, J. H. *Science* **1981**, *214*, 1081.

(5) (a) Casado-Rivera, E.; Gal, Z.; Angelo, A. C. D.; Lind, C.; DiSalvo, F. J.; Abruna, H. D. *ChemPhysChem* **2003**, *4*, 193. (b) Casado-Rivera, E.; Volpe, D. J.; Alden, L.; Lind, C.; Downie, C.; Valzquez-Alvarez, T.; Angelo, A. C. D.; DiSalvo, F. J.; Abruna, H. D. *J. Am. Chem. Soc.* **2004**, *126*, 4043. (c) Mathauser, A. T.; Teplyakov, A. V. *Catal. Lett.* **2001**, *73*, 207. (d) Bauer, J. C.; Chen, X.; Liu, Q.; Phan, T.-H.; Schaak, R. E. *J. Mater. Chem.* **2008**, *18*, 275. (e) Wee, J. H.; Lee, K. Y. *J. Power Sources* **2006**, *157*, 128. (f) Liu, Z. L.; Guo, B.; Hong, L.; Lim, T. H. *Electrochem. Commun.* **2006**, *8*, 83.

(6) (a) Hassoum, J.; Panero, S.; Scrosati, B. *J. Power Sources* **2006**, *160*, 1336. (b) Hassoum, J.; Panero, S.; Simon, P.; Taberna, L.; Scrosati, B. *Adv. Mater.* **2007**, *19*, 1632. (c) Jiang, T.; Zhang, S. C.; Qiu, X. P.; Zhu, W. T.; Chen, L. Q. *J. Power Sources* **2007**, *166*, 503. (d) Mladenv, M.; Zlatilova, P.; Drajieva, I.; Klabunde, K. *J. Power Sources* **2006**, *162*, 803. (e) Sarakonsri, T.; Apirattanawan, T.; Tungprasurt, S.; Tunkasiri, T. *J. Mater. Sci.* **2006**, *41*, 4749.

10.1021/cm703640u CCC: $40.75

nanocrystals with predominantly spherical and cubic shapes can also be generated using these methods.[13] However, unlike previous reports, here we establish general and predictive guidelines for accessing single-crystal nanorods in a large number of chemically distinct intermetallic systems. We also demonstrate the ability to selectively generate hollow vs dense nanorods, including within the same system. The formation of one-dimensional nanostructures of these compounds using a unified and materials-general method is significant, because the target systems represent a diverse range of useful materials that have known dimension- and size-dependent properties, including superconducting AuSn,[14] catalytically active PtSn,[5e,f] and Ni_3Sn_4 and Cu_6Sn_5 with Li insertion capabilities for battery applications.[6]

Experimental Section

Chemicals. The following metal reagents were used: $SnCl_2$ (anhydrous, 99% min.), $CoCl_2 \cdot 6H_2O$ (98.0–102%), $NiCl_2 \cdot 6H_2O$ (99.95%), $Cu(NO_3)_2 \cdot 3H_2O$ (98.0–102%), $RuCl_3 \cdot 6H_2O$ (99.9%), $HAuCl_4 \cdot 3H_2O$ (Au 49.5% min), K_2PtCl_6 (Pt 40.11%), and $AgNO_3$ (99.9+%). The reducing agent, surface stabilizer, and solvent were $NaBH_4$ (98%), poly(vinyl pyrrolidone) (PVP, MW = 630 000), tetraethylene glycol (TEG, 99+%), and ethylene glycol (EG, 99+%), respectively. All chemicals were purchased from Alfa Aesar and used as received.

Synthesis of *β*-Sn Nanorods. *β*-Sn nanorods, used as templates, were synthesized in a manner similar to that of our previous report.[13] First, 0.4 g of PVP (MW = 630 000) was dissolved in 45 mL of TEG at room temperature. $SnCl_2$ (0.08 g in 4 mL of TEG) was added, along with a freshly prepared solution of $NaBH_4$ (0.264 g in 8 mL of TEG) while stirring. The temperature was gradually increased to 100 °C over 40 min. Concurrently, *β*-Sn seed nanocrystals were prepared by sequentially adding 0.25 g of PVP, 0.05 g of $SnCl_2$, and 0.16 g of $NaBH_4$ to 20 mL of TEG at room temperature. This solution of *β*-Sn seed nanocrystals was added to the original *β*-Sn nanocrystal solution at 100 °C and then heated to 160 °C for 1 h. The temperature was then increased to 190 °C, and the solution was removed from the heat. The predominately rod-shaped *β*-Sn nanocrystals were isolated by centrifugation and washed with ethanol.

Synthesis of Intermetallic Nanorods. To synthesize intermetallic M−Sn (M = Co, Ni, Au, Cu, Ag, Ru, Pt) nanocrystals at different reaction temperatures, the temperature of the solution of *β*-Sn seed nanocrystals was adjusted for the desired reaction temperature after synthesizing *β*-Sn nanorods. After reaching the desired reaction temperature, the appropriate metals salts were added to the solution of *β*-Sn seed nanocrystals: $CoCl_2 \cdot 6H_2O$ (0.29 mmol, 0.07 g in 5 mL of TEG at 150 °C or above as described in the text), $NiCl_2 \cdot 6H_2O$ (0.336 mmol, 0.08 g in 5 mL of TEG at 150 °C), $HAuCl_4 \cdot 3H_2O$ (0.25 mmol, 0.098 g in 5 mL of TEG at 150 °C and 0.35 mmol, 0.137 g in 5 mL of TEG at room temperature and 0 °C), $Cu(NO_3)_2 \cdot 3H_2O$ (0.175 mmol, 0.042 g in 5 mL of TEG at 150 °C and 0.25 mmol, 0.07 g in 5 mL of TEG at room temperature and 0 °C), and $AgNO_3$ (0.2 mmol, 0.0339 g in 5 mL of TEG at 150 °C and 0.2 mmol, 0.0339 g in 5 mL of TEG at room temperature and 0 °C). For $RuSn_2$ and PtSn, the temperature of the *β*-Sn nanorod solution was held at 190 °C, then sequentially $RuCl_3 \cdot 6H_2O$ (0.3 mmol, 0.06 g in 5 mL of EG, ethylene glycol) and K_2PtCl_6 (0.35 mmol, 0.17 g in 10 mL of EG) were added to the solution of *β*-Sn nanorods. The temperature was then increased to 200 and 290 °C, respectively. After reaching the desired temperature, the temperature was held for 30 min.

Characterization. X-ray diffraction (XRD) data were collected on a Bruker GADDS three-circle X-ray diffractometer using Cu Kα radiation. Transmission electron microscopy (TEM) images, selected area electron diffraction (SAED) patterns, and energy-dispersive X-ray analysis (EDS) were collected using a JEOL JEM-2010 TEM. Samples were prepared by sonicating the nanocrystalline intermetallic powders in ethanol and dropping a small volume onto a carbon-coated nickel or copper grid.

Results and Discussion

Single-crystal nanorods of *β*-Sn (~72% yield with additional spheres present) were synthesized using a multistep seed-mediated strategy involving the reaction of $SnCl_2$ with $NaBH_4$ in tetraethylene glycol (TEG) in the presence of poly(vinylpyrrolidone) (PVP). These *β*-Sn nanocrystals (see Supporting Information), while not perfectly uniform in size or shape purity, are among the best reported in the literature for *β*-Sn in this size range[15] and are of sufficient quality to draw meaningful conclusions from the studies that follow. When reacted with optimized amounts of appropriate metal salt solutions and excess $NaBH_4$ in TEG at temperatures of 150 °C or higher, the *β*-Sn nanorods cleanly convert to nanocrystalline M−Sn (M = Co, Ni, Cu, Ag, Au, Pt, Ru) intermetallic compounds, based on the XRD data shown in Figure 1 and in Supporting Information. Interestingly, $RuSn_2$ is an elusive compound in bulk systems, described in the literature as a metastable phase that does not appear on the equilibrium Ru−Sn phase diagram and one that is difficult to access synthetically and stabilize.[16] $RuSn_2$ appears to form reproducibly using this template-based synthetic strategy.

---

(7) (a) Wiley, B.; Sun, Y.; Xia, Y. *Acc. Chem. Res.* **2007**, *40*, 1067. (b) Gou, L.; Murphy, C. *J. Chem. Mater.* **2005**, *17*, 3668. (c) Jun, Y.-W.; Choi, J.-S.; Cheon, J. *Angew. Chem., Int. Ed.* **2006**, *45*, 3414. (d) Yin, Y.; Alivisatos, A. P. *Nature* **2005**, *437*, 664. (e) Scher, E. C.; Manna, L.; Alivisatos, A. P. *Philos. Trans. R. Soc. London, Ser. A* **2003**, *361*, 241.

(8) Maksimuk, S.; Yang, S.; Peng, Z.; Yang, H. J. *J. Am. Chem. Soc.* **2007**, *129*, 8684.

(9) (a) Gates, B.; Wu, Y.; Yin, Y.; Yang, P.; Xia, Y. *J. Am. Chem. Soc.* **2001**, *123*, 11500. (b) Gates, B.; Mayers, B.; Wu, Y.; Sun, Y.; Cattle, B.; Yang, P.; Xia, Y. *Adv. Funct. Mater.* **2002**, *12*, 679. (c) Jeong, U.; Camargo, P. H. C.; Lee, Y. H.; Xia, Y. *J. Mater. Chem.* **2006**, *16*, 3893.

(10) (a) Yin, Y.; Rioux, R. M.; Erdonmez, C. K.; Hughes, S.; Somorjai, G. A.; Alivisatos, A. P. *Science* **2004**, *304*, 711. (b) Yin, Y.; Erdonmez, C. K.; Cobot, A.; Hughes, S.; Alivisatos, A. P. *Adv. Funct. Mater.* **2006**, *16*, 1389.

(11) (a) Chiang, R.-K.; Chiang, R.-T. *Inorg. Chem.* **2007**, *46*, 369. (b) Henkes, A. E.; Vasquez, Y.; Schaak, R. E. *J. Am. Chem. Soc.* **2007**, *129*, 1896. (c) Henkes, A. E.; Schaak, R. E. *Chem. Mater.* **2007**, *19*, 4234. (d) Henkes, A. E.; Schaak, R. E. *Inorg. Chem.* **2008**, *47*, 671–677.

(12) (a) Fan, H. J.; Knez, M.; Scholz, R.; Hesse, D.; Nielsch, K.; Zacharias, M.; Gosele, U. *Nano Lett.* **2007**, *7*, 993. (b) Fan, H. J.; Knez, M.; Scholz, R.; Nielsch, K.; Pippel, E.; Hesse, D.; Zacharias, M.; Gosele, U. *Nat. Mater.* **2006**, *5*, 627. (c) Lin, B.; Zeng, H. C. *J. Am. Chem. Soc.* **2004**, *126*, 16744. (d) Fan, H. J.; Gosele, U.; Zacharias, M. *Small* **2007**, *3*, 1660.

(13) Chou, N. H.; Schaak, R. E. *J. Am. Chem. Soc.* **2007**, *129*, 7339.

(14) Hamilton, D. C.; Raub, Ch., J.; Matthias, B. T. *J. Phys. Chem. Solids.* **1965**, *26*, 665.

(15) (a) Hsu, Y.-J.; Lu, S.-Y. *J. Phys. Chem. B* **2005**, *109*, 4398. (b) Hsu, Y.-J.; Lu, S.-Y.; Lin, Y.-F. *Small* **2006**, *2*, 268. (c) Nayral, C.; Viala, E.; Fau, P.; Senocq, F.; Jumas, J.-C.; Maisonnat, A.; Chaudret, B. *Chem. Eur. J.* **2006**, *6*, 4082.

(16) (a) Massalski, T. B., Ed. *Binary Alloy Phase Diagrams*; ASM International: Materials Park, OH, 1996. (b) Ananthasivan, K.; Kaliappan, I.; Rao, P. R. V.; Sudha, C.; Terrance, A. L. E. *J. Nucl. Mater.* **2002**, *305*, 97.

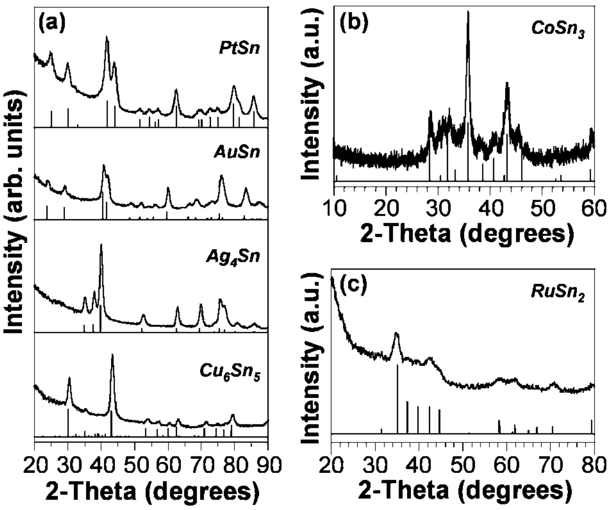

Figure 1. Powder XRD patterns for nanocrystalline intermetallics formed by reacting β-Sn nanocrystals with appropriate metal salt solutions under reducing conditions. (a) PtSn, AuSn, Ag_4Sn, and Cu_6Sn_5, (b) $CoSn_3$, and (c) $RuSn_2$. Top: experimental. Bottom: patterns from PDF card 25–0614 (PtSn); 8–0463 (AuSn); 29–1151 (Ag_4Sn); 45–1488 (Cu_6Sn_5); 48–1813 ($CoSn_3$); 51–0741 ($RuSn_2$).

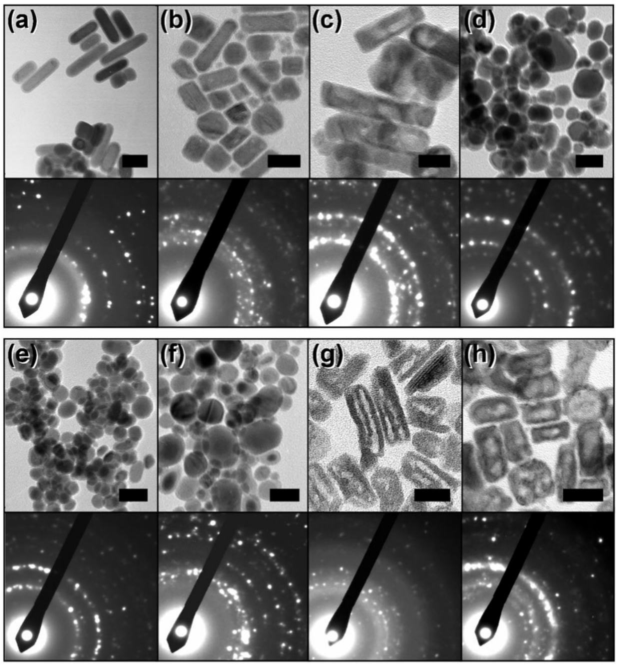

Figure 2. TEM micrographs and SAED patterns of nanocrystalline (a) β-Sn, (b) $CoSn_3$, (c) Ni_3Sn_4, (d) AuSn, (e) Cu_6Sn_5, (f) Ag_4Sn, (g) $RuSn_2$ (200 °C), and (h) PtSn (290 °C). All reactions were carried out at 150 °C unless otherwise noted. Scale bars are 20 nm.

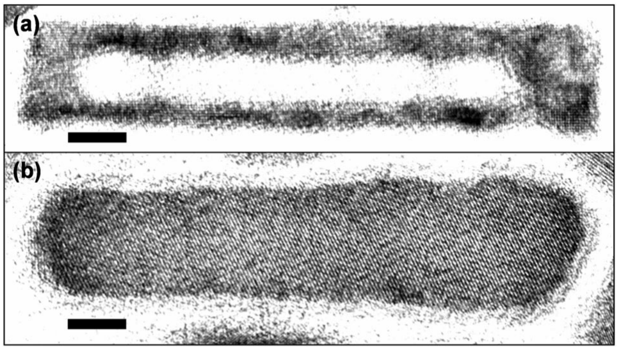

Figure 3. High resolution TEM micrographs of (a) hollow single-crystal Ni_3Sn_4, nanorods and (b) dense single-crystal $CoSn_3$ nanorods. Scale bars are 5 nm.

Despite the fact that the conversion reactions cleanly yield *M*-Sn intermetallics, the transmission electron microscopy (TEM) images in Figure 2 show clear differences in the morphologies of the intermetallic nanocrystal products. When reacted with $CoCl_2 \cdot 6H_2O$ at 150 °C, the β-Sn nanorod templates form predominantly dense $CoSn_3$ nanorods. When reacted with $NiCl_2 \cdot 6H_2O$ at 150 °C, however, Ni_3Sn_4 forms a mixture of dense (minor product) and hollow (major product) nanorods. Similar reactions of β-Sn nanorods with $Cu(NO_3)_2 \cdot 3H_2O$, $AgNO_3$, and $HAuCl_4 \cdot 3H_2O$ at 150 °C form Cu_6Sn_5, Ag_4Sn, and AuSn intermetallics, respectively, with dense spherical morphologies rather than nanorod shapes. Finally, reactions of β-Sn nanorods with $RuCl_3 \cdot xH_2O$ at 200 °C and K_2PtCl_6 at 290 °C (the minimum temperatures necessary to form the desired Ru and Pt intermetallic products) produce hollow nanorods of $RuSn_2$ and PtSn, respectively, with no dense nanorods observed. For the systems that yield intermetallic nanorods, the yield of nanorods is always between 65 and 70%, which agrees well with the percentage of nanorods in the β-Sn precursor samples (~72%) and indicates that a large majority of the nanorods are converted with shape retention. Selected area electron diffraction (SAED) patterns, included in Figure 2, confirm the formation of intermetallic nanocrystals in all of the *M*−Sn systems, since these compounds are line phases that have narrow composition windows and composition-dependent crystal structures that differ from their constituent elements. The intermetallic nanorods produced from these reactions are generally single crystals, as shown for hollow nanorods of Ni_3Sn_4 (Figure 3) and PtSn (Supporting Information) and dense nanorods of $CoSn_3$ (Figure 3b).

Building on this observation, the Cu−Sn system was studied in detail. When reacted with $CuCl_2 \cdot 3H_2O$ at 150 °C, β-Sn nanorods convert to Cu_6Sn_5. However, the nanorod morphology is destroyed and the products are exclusively spherical nanocrystals (Figure 2e), which represent the equilibrium nanocrystal shapes that form via direct synthesis without the use of shape-controlled templates. When the reaction is carried out at room temperature, spherical Cu_6Sn_5 nanocrystals are also formed (Figure 5a). However, when cooled to 0 °C, the nanorod shape is retained, generating single-crystal intermetallic Cu_6Sn_5 nanorods (panels b and e in Figure 5). Likewise, when β-Sn nanorods are reacted with $HAuCl_4 \cdot 3H_2O$ and $AgNO_3$ at 0 °C, single-crystal AuSn (panels d and f in Figure 5), and Ag_4Sn (Figure 5g) nanorods, respectively, are formed. This is in contrast to the AuSn and Ag_4Sn nanospheres that form at 150 °C (panels d and f in Figure 2) and room temperature (Figure 5c). Thus, for the systems that initially appeared unable to retain the morphology defined by the β-Sn nanorod templates, using a significantly lower reaction temperature facilitated morphological retention and yielded single-crystal nanorods. These results demonstrate that single-crystal intermetallic nanorods are accessible in all of the *M*−Sn systems studied using a single unified process, and imply that conditions could be identified to expand the library of intermetallic nanorods to include many other systems.

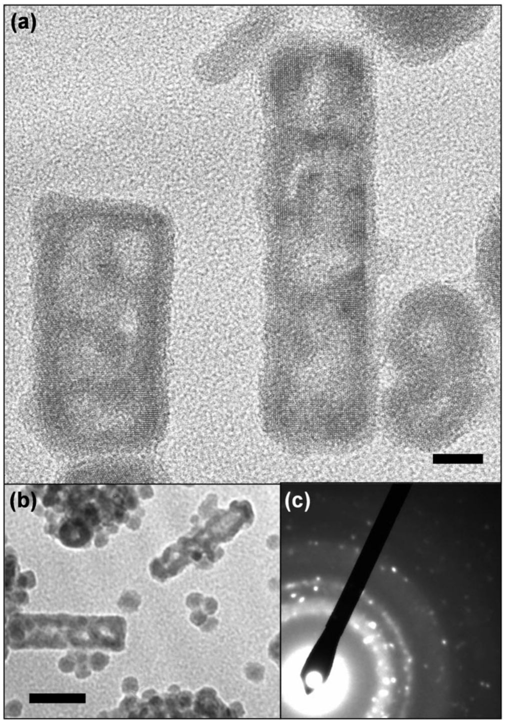

Figure 4. TEM micrographs of (a) hollow single-crystal $CoSn_3$ nanorods and (b) a larger-view image showing the beginning of fragmentation into smaller spherical nanoparticles. The corresponding SAED pattern is shown in (c). Scale bars are 20 nm.

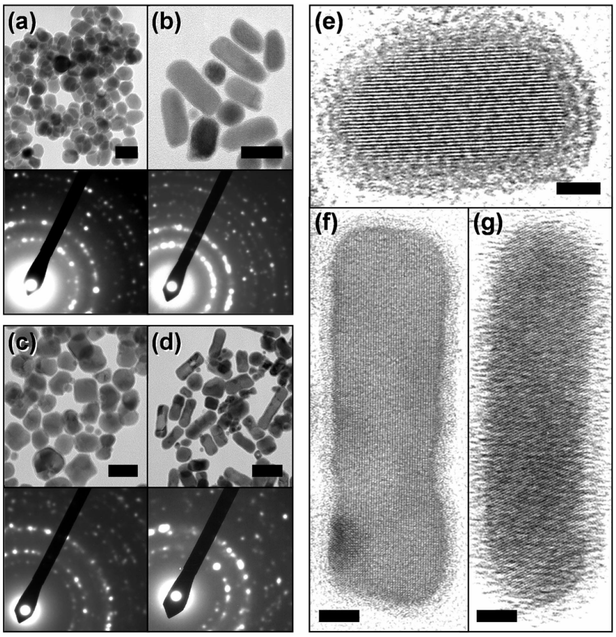

Figure 5. TEM micrographs and SAED patterns for (a) predominantly spherical Cu_6Sn_5 at ~20 °C, (b) single-crystal Cu_6Sn_5 nanorods at 0 °C, (c) predominantly spherical AuSn at ~20 °C, (d) single-crystal AuSn nanorods at 0 °C, and high-resolution TEM micrographs for single-crystal nanorods of (e) Cu_6Sn_5, (f) AuSn, and (g) Ag_4Sn. Scale bars are 20 nm in (a−d) and 5 nm in (e−g).

The results presented above can be combined to yield a self-consistent and predictive set of guidelines for rationally generating morphology-controllable intermetallic nanocrystals, and also for understanding the conditions under which intermetallic nanocrystals can be synthesized using diffusion-based template approaches. As one would predict, temperature plays a primary role in the formation of intermetallic nanocrystals, as well as the ability to retain the morphology of the β-Sn nanocrystal templates. The process that converts β-Sn nanorods to M−Sn nanorods is a diffusion-based process, and diffusion is a temperature-dependent phenomenon.[17,18] The melting point of an element can serve as a rough estimate of its rate of diffusion relative to that of other elements.[18] This is useful for establishing qualitative and empirical guidelines for differences in reactivity among several comparable systems, especially considering the inherent complexity of nanoscale diffusion phenomena.[12d] Accordingly, the melting points of the transition elements used in this study define three diffusion categories (melting points, in °C,[19] are in parentheses): (a) fast diffusers Ag (961), Au (1064), Cu (1084); (b) moderate diffusers Ni (1455), Co (1495); and (c) slow diffusers Pt (1768), Ru (2334). The fast diffusers, which are known to have diffusion rates a few orders of magnitude greater than self-diffusion (e.g., Sn in Sn),[20] diffuse so fast that they destroy the template, precluding shape retention. Cooling the reaction sufficiently low to slow down diffusion in these systems facilitates shape retention, yielding single-crystal nanorods. The moderate diffusers are able to retain shape at moderate temperatures (~150 °C), with some remaining dense and others becoming hollow. Finally, the slow diffusers do not completely diffuse into the β-Sn nanocrystal templates until higher temperatures (>200 °C), precluding the formation of intermetallic compounds at lower temperatures. Since their diffusion into the β-Sn nanocrystal templates is slow relative to the rate of outward Sn diffusion, voids are created in the center of the nanorods, generating hollow nanorods via a nanoscale Kirkendall effect.[9–13]

In addition to providing guidelines relevant to morphology control, these results also provide insight into understanding the lowest temperatures that intermetallic compounds can form using low-temperature solution chemistry routes. For example, the low-melting fast diffusers (Ag, Au, Cu) can form M−Sn intermetallics at or below room temperature. The high-melting slow diffusers (Pt, Ru) do not react with Sn at room temperature, and require significantly higher temperatures (>200 °C) to form intermetallics. The intermediate melting and diffusing elements (Fe, Ni, Co) do not form intermetallics at room temperature, but react with Sn at moderate temperatures (~150 °C) to form intermetallics. This understanding, when coupled with the growing library of intermetallic compounds that are accessible as nanocrystals using similar routes,[21] could aid our synthetic efforts and further expand our ability to generate nanocrystalline intermetallics on-demand in a variety of other systems.

---

(17) Dienes, G. J. *J. Appl. Phys.* **1950**, *21*, 1189.

(18) Mehrer. H. *Diffusion in Solids*; Springer: New York, 2007.

(19) Hammond, C. R. In *Handbook of Chemistry and Physics*, 74th ed.; CRC Press: Boca Raton, FL, 1993; pp 4–36..

(20) (a) Dyson, B. F. *J. Appl. Phys.* **1966**, *37*, 2375. (b) Dyson, B. F.; Anthony, T. R.; Turnbull, D. *J. Appl. Phys.* **1967**, *38*, 3408. (c) Nowick, A. S.; Burton, J. J. In *Diffusion in Solids*−*Recent Developments*; Academic Press, New York, 1975.

(21) (a) Sra, A. K.; Ewers, T. D.; Schaak, R. E. *Chem. Mater.* **2005**, *17*, 758. (b) Cable, R. E.; Schaak, R. E. *Chem. Mater.* **2005**, *17*, 6835. (c) Cable, R. E.; Schaak, R. E. *J. Am. Chem. Soc.* **2006**, *128*, 9588. (d) Leonard, B. M.; Schaak, R. E. *J. Am. Chem. Soc.* **2006**, *128*, 11475. (e) Cable, R. E.; Schaak, R. E. *Chem. Mater.* **2007**, *19*, 4098.

Conclusions

In summary, we have shown that a library of single-crystal *M*−Sn intermetallic nanorods can be synthesized by exploiting the diffusion characteristics of the reacting metals. This information (relative diffusion rates estimated from melting points), which is well-established in bulk and thin film systems,[18] can be used as a predictive guideline in nanocrystal systems for establishing optimal reaction temperatures that (a) maintain the morphologies of the Sn nanocrystal templates (e.g., preferentially access spheres vs nanorods), (b) generate dense vs hollow nanorods via a nanoscale Kirkendall effect, and (c) allow one to estimate the relative minimum temperatures necessary for forming intermetallic compounds using low-temperature solution routes. This understanding, and its ability to be applied as a unified synthetic strategy in a practical and general manner, is important for advancing the morphology-controlled synthesis of a large number of technologically relevant intermetallic and other multielement nanocrystals using robust diffusion-based strategies.

Acknowledgment. This work was supported by the National Science Foundation (DMR-0545201 and DMR-0748943), the Robert A. Welch Foundation (Grant A-1583), DuPont (Young Professor Grant), and the Arnold and Mabel Beckman Foundation (Young Investigator Award). Acknowledgement is also made to the donors of the Petroleum Research Fund, administered by the American Chemical Society. Electron microscopy was performed at the Microscopy and Imaging Center at Texas A&M University, and XRD data were collected at the X-ray Diffraction Laboratory in the Department of Chemistry at Texas A&M University.

Supporting Information Available: XRD data for β-Sn and Ni_3Sn_4 nanocrystals; larger-area TEM micrographs for AuSn, $RuSn_2$, and β-Sn nanorods; and HRTEM micrographs of hollow single-crystal PtSn and $CoSn_3$ nanorods (PDF). This material is available free of charge via the Internet at http://pubs.acs.org.

CM703640U